AN ANALYSIS OF A SHALLOW COLD FRONT AND WAVE INTERACTIONS FROM THE PLOWS FIELD CAMPAIGN

P.105

Carter Hulsey and Kevin Knupp
Severe Weather Institute and Radar & Lightning Laboratories, University of Alabama in Huntsville, Huntsville, AL

1. INTRODUCTION

The Profiling of Winter Storms (PLOWS) field campaign IOP-19 occurred February 14-15, 2010. During this IOP a shallow cold front associated with a weak cyclone moved through southern Indiana and was followed by and upper level boundary as well as a secondary but weaker cold front. Several wave features were also seen during the IOP after the passage of the shallow cold front. This paper present the impact of the front and wave features on the enchantment of precipitation over southern Indiana during IOP 19.

2. Instrumentation Array Setup

The PLOWs mobile platforms were set up in a linear orientation from 250 to 70 degrees with the MISS located to the southwest endpoint, MAX at the center, and MIPS at the northeast endpoint (Figure 1). The mobile platforms were separated by a distance of 47 and 15 km, respectively. The mobile platforms included the NCAR Mobile Integrated Sounding System (MISS; 915 MHz wind profiler and soundings), the Mobile Alabama X-band (MAX) dual polarization radar (including surface measurements), and the UAH Mobile Integrated Profiling System (MIPS; 915 MHz wind profiler, X-band profiling radar, microwave profiling radiometer, ceilometer, surface instrumentation, and Parsivel disdrometer). During the IOP the Wyoming cloud radar on the NCAR C-130 sampled along the mobile platform line. The phenomena of interest were also sampled by the Evansville, Indiana, WSR-88D radar (KVWX) as well as surface station (AWOS and Co-op) within the PLOWS IOP 19 domain.

3. Frontal Passage Through the Domain.

The shallow cold front moved through the domain from the southwest moving toward the northeast. The front had a wind shift from 155 to 270 degrees, 6-8°C temperature reduction, shallow depth (< 1km), and significant pressure rise (1.5 hPa). All changes occurred within an approximate 30 minute time period with the most significant changes occurring within 15 minutes (Figure 2). The shallow front acted similar to that of a density current which is a layer of colder air that pushes under and lifts a warmer air mass above it leading to CI or enhancement in precipitation (Seitter 1986). Density currents are associated with pressure rises, temperature drops, and dewpoint rises at the surface as can be seen in the surface instrumentation at MISS and MAX (Figure 2).

The shallow cold front passed over the MISS at around 0330 UTC. The MISS 915 MHz 30 minute consensus wind profiles (Figure 3) shows a shift in the wind from south too stronger westerly after the passage of the front. The wind shift caused by the frontal passage is limited to the lowest 1km AGL, with winds above 1km remaining mostly unaffected by the shallow frontal passage. Post frontal winds at the MISS proceeded to strengthen from 5 to 8 m/s. The MISS 915 SNR (Figure 4) showed a distinct low level maximum around the time of frontal passage signifying a local augmentation in precipitation. The MISS 915 vertical motion (Figure 4) showed predominantly downward motion before the passage of the shallow cold front and the downward motion persisted after its passage until 0345 UTC. Downward motion persisted after this however areas of upward vertical velocity could be seen oscillating with downward motion at 5-6 km AGL from 0350-0600 UTC.

The shallow cold front passed over the MIPS site at approximately 0510 UTC. The 915 MHz 30 minute consensus wind profiles at MIPS (Figure 5) showed a wind shift from south southwest to west and an increase of 5-7 m/s in the lowest 1 km as the shallow front passed. The 915 SNR and Vertical motion (Figure 6) shows a perturbation in vertical motion as the front passed and strengthened downward motion after frontal passage. The front was well sampled by the MIPS MPR (Figure 7.) and showed a drop in temperature of 4°C, drop of 6°C in theta v, and decrease of .00015 kg/kg in mixing ratio. The MIPS XPR (Figure 8) had an increase in Reflectivity as the front passed. Downward vertical motion increased below 1km after the frontal passage.

During IOP 19 the MAX radar was performing PPI scans from 1 to 60 degrees with

RHIs along the C-130 flight line between MISS and MIPS. RHI's from max before the frontal passage (Figure 9) show relatively shallow and weak precipitation ahead of the front. Values of the more moderate reflectivity only reached up to around 2 km AGL. The front was able to be seen in the RHI's as an area of deeper moderate reflectivity with a depth of 4-6 km. The front passed over the MAX site around 0510 UTC. Post frontal RHI's (Figure 10) showed a deeper and stronger area of higher reflectivity with a depth of 4 km and peak value of 20 dBZ.

3. Post Shallow Cold Front Phenomena

The feeder flow after the shallow cold front passage shifted the low level winds at the MISS to the northwest (Figure 3) while staying westerly as MIPS (Figure 4).

The MIPS MPR (Figure 7) showed am upper level boundary that passed over the domain approximately two and a half hours after the initial shallow cold front. The upper level boundary only affected the atmosphere above 1.5 km AGL. The upper level boundary was associated with a 2-3°C drop in temperature, a 6°C drop in theta v, and a very small decrease in mixing ratio. The secondary upper level boundary was associated with another enhancement in reflectivity more significant than the initial surface based shallow cold front. The upper level front precipitation enhancement was seen with an increase in XPR reflectivity (Figure 8).

After the passage of the shallow cold front there were passages of wave life features through the IOP domain. The wave features were supported by a stable layer over the depth of the front. The prefrontal soundings at the MISS site show a stable layer over the front depth with lapse rates of 4-5°C/km. The wave features were first seen in the MISS 915 MHz Wind profiler vertical motion field. The wave features were seen in areas of upward vertical velocity that were oscillating with downward motion at 5-6 km AGL from 0350-0600 UTC. The upward motion vertical velocities began to stretch downward to 2-2.5km AGL from 0600-0800 UTC. This time period showed the strongest upward motion at 1.5 m/s as well as the strongest downward motion at -2.0 m/s. The oscillations continued through the rest of the period. These oscillations are associated with the passage of post frontal wave features that were also seen at the MIPS and MAX sites. These wave features could be seen in the MIPS XPR (Figure 8). The wave features in XPR could be seen through reflectivity perturbations as well as oscillation in the vertical motion. The wave features were observed from 0400-0800 UTC in the XPR. The vertical extent of the velocity oscillations were from 3.5-7.0 km AGL with peak upward motions of 1.5-2.0 m/s. The post frontal waves were also well sampled by the MAX radar. Looking at the post frontal RHI's (Figure 10) perturbation in reflectivity can be seen in the stable layer above the depth of the previous frontal passage.

Another surface based cold front passed through the region around 9-10 hours after the initial shallow cold front passed. This front was much weaker only seeing around a 2°C drop in Temperature and a 3°C drop in dewpoint at the surface station sites within the IOP 19 domain.

4. Conclusions and Future Work

On February 14-15th, 2010, IOP 19 of the PLOWS field campaign sampled a shallow cold front and associated wave features that moved through the domain. The front and features were well sampled by the mobile platforms as well as the Evansville, Indiana, WSR-88D and surface stations within the IOP domain. The shallow front had density current like attributes and acted as a density current leading to an enhancement in the precipitation. The front was associated with wave like features that propagated in a stable layer after the frontal passage. A secondary upper level boundary sampled by the MIPS MPR (Figure 7) shows a decrease in temperature above 1.5 km associated with another enhancement in precipitation. A second cold front then passed through the IOP domain at 9-10 hours after the initial shallow cold front.

Future work will include a wave analysis using the MISS site sounding data to find Richardson number and vertical wavelength (m^2) (Scorer 1949; Coleman and Knupp 2008). NIMA reprocessing will be done on the 915 MHz wind profiler data at both MISS and MIPS to get 10 minute wind profiles (Morse et al. 2002). A 2-D single Doppler analysis will be performed using the MAX radar to see the flow field around the shallow cold front.

5. References

Timothy A. Coleman and Kevin R. Knupp, 2008: The Interactions of Gravity Waves with Mesocyclones: Preliminary Observations and Theory. Mon. Wea. Rev., 136, 4206–4219.

Corinne S. Morse, Robert K. Goodrich, and Larry B. Cornman, 2002: The NIMA Method for Improved Moment Estimation from Doppler Spectra. J. Atmos. Oceanic Technol., 19, 274–295.

Scorer, R., 1949: Theory of waves in the lee of mountains. Quart. J. Roy. Meteor. Soc., 75, 41–56.

Keith L. Seitter, 1986: A Numerical Study of Atmospheric Density Current Motion Including the Effects of Condensation. J. Atmos. Sci., 43, 3068–3076.

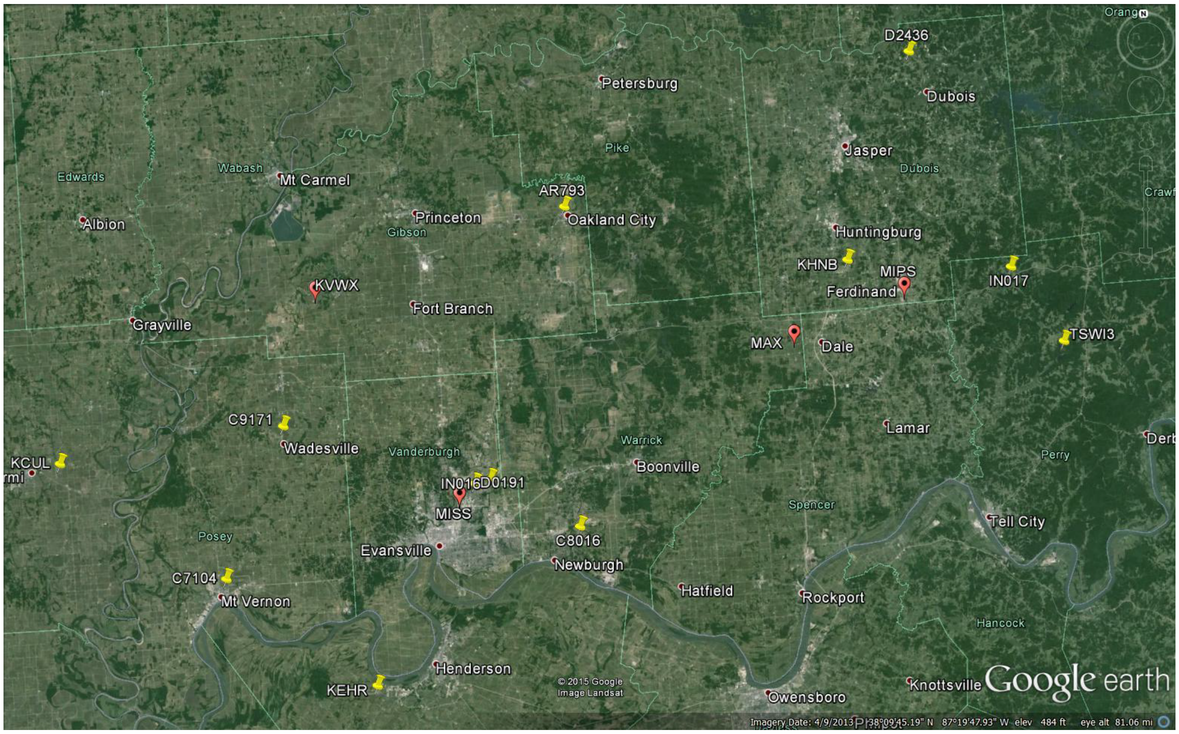

Figure 1: Maps image of IOP 19 domain. Surface stations are marked yellow. KVWX, the mobile platforms are marked red, and distance between instruments in black.

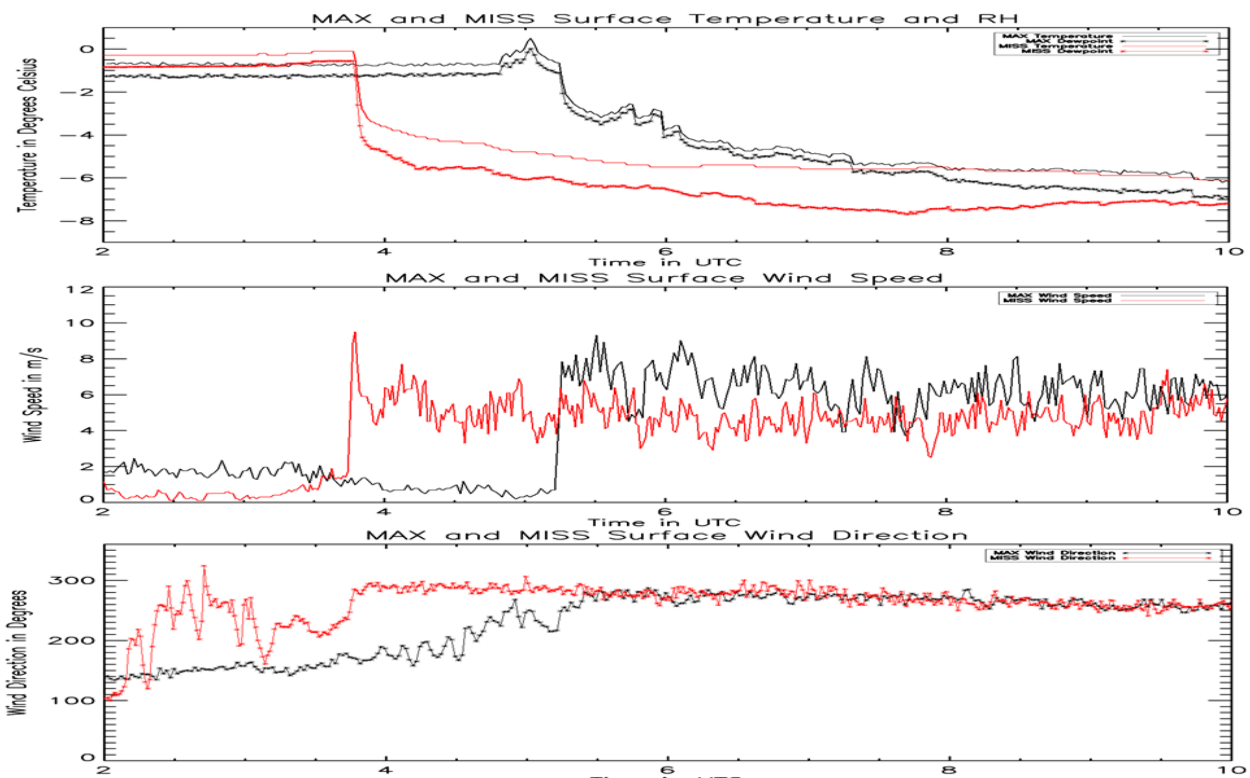

Figure 2: MAX and MISS surface station plot of temperature, dewpoint, pressure, wind direction, wind speed, and wind gusts on February 15th, 2010 from 0200-1000 UTC.

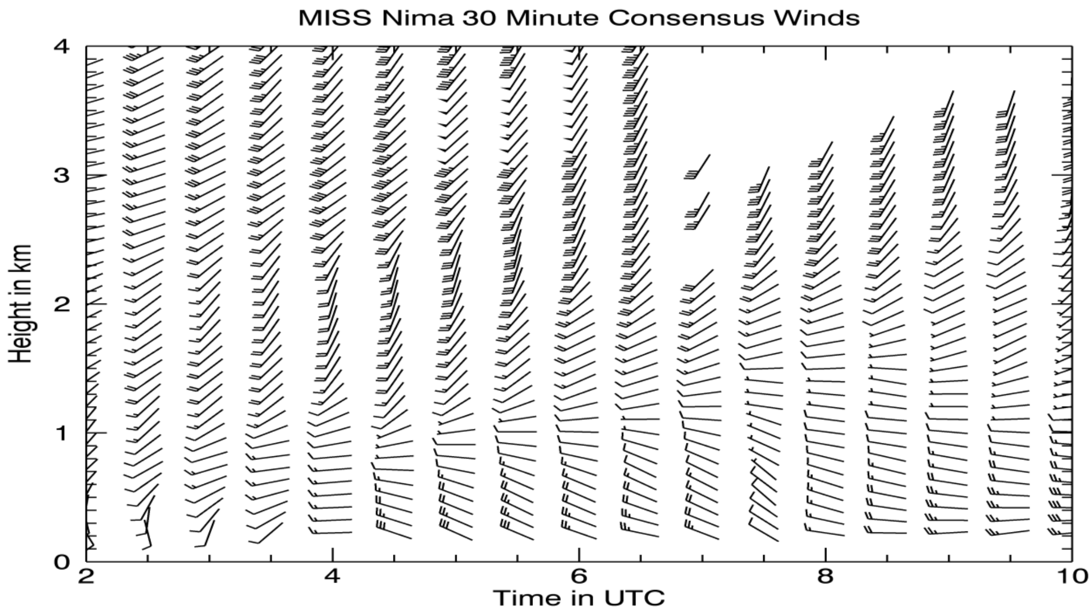

Figure 3: MISS 915 MHz wind profiler 30 minute consensus wind profile from 0200-1000 UTC on the 15th. Frontal passage occurred at 0345 UTC with a depth of around 1km.

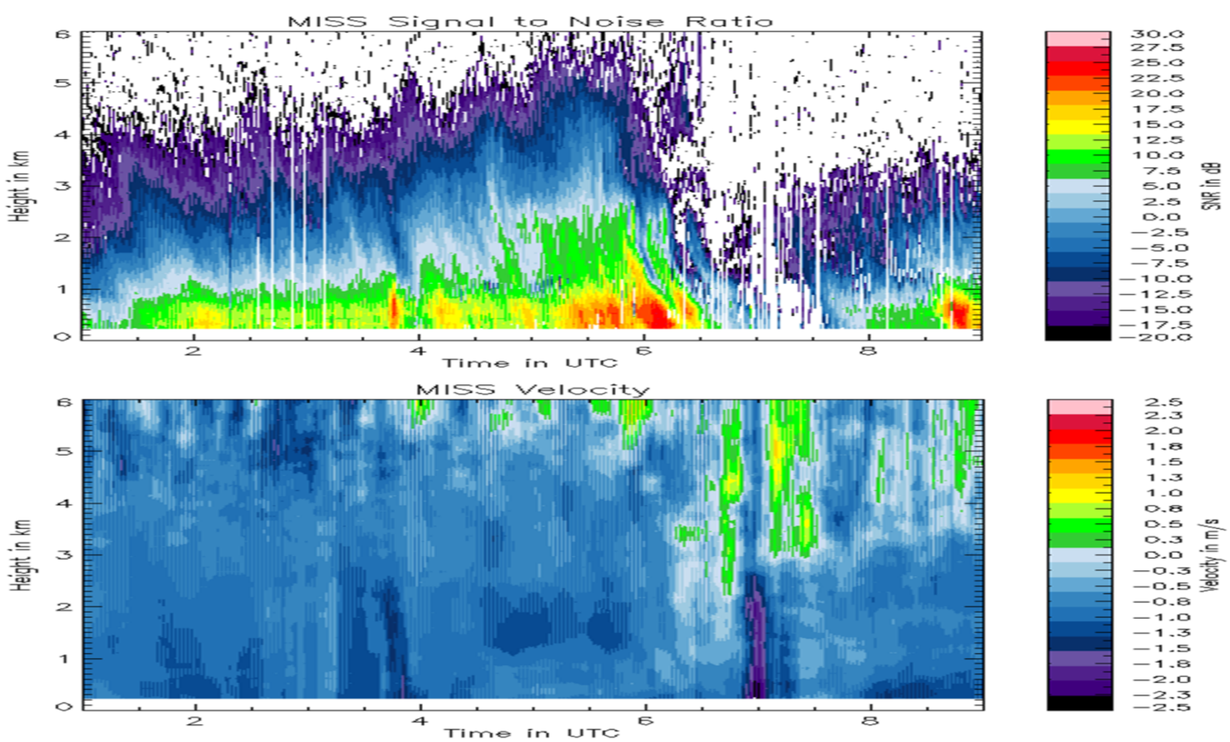

Figure 4: MISS 915 MHz wind profiler SNR and vertical motion from February 15th from 0100-0900 UTC. Frontal Passage occurring at 0345 UTC

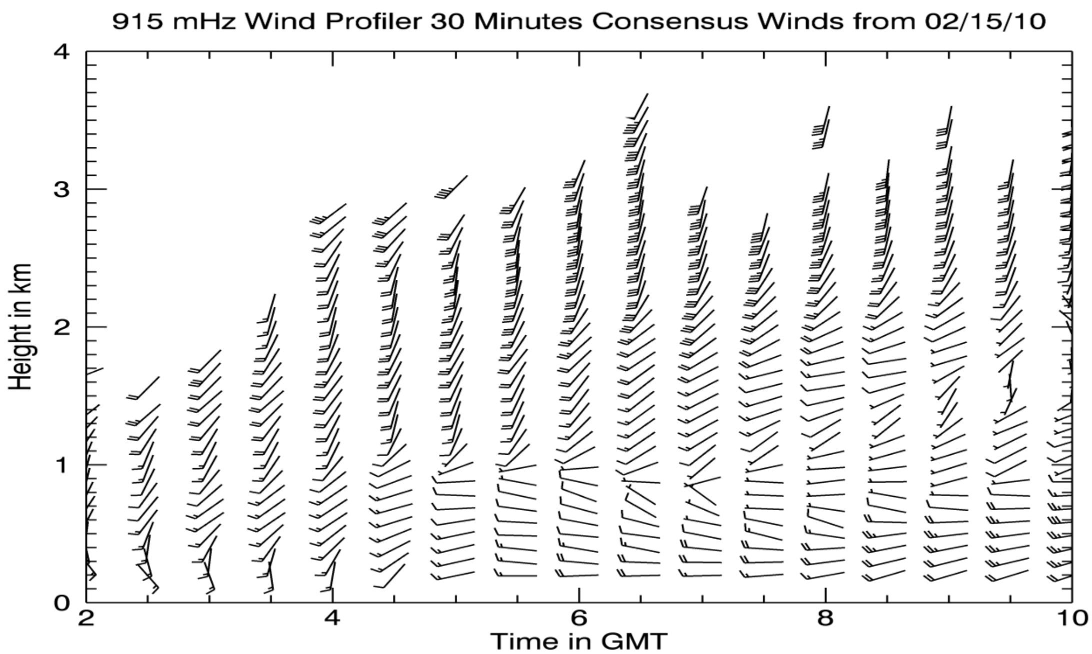

Figure 5: MIPS 915 MHz wind profiler 30 minute consensus wind profile from 0200-1000 UTC on the 15th. Frontal passage occurred at 0515 UTC with a depth of around 1km.

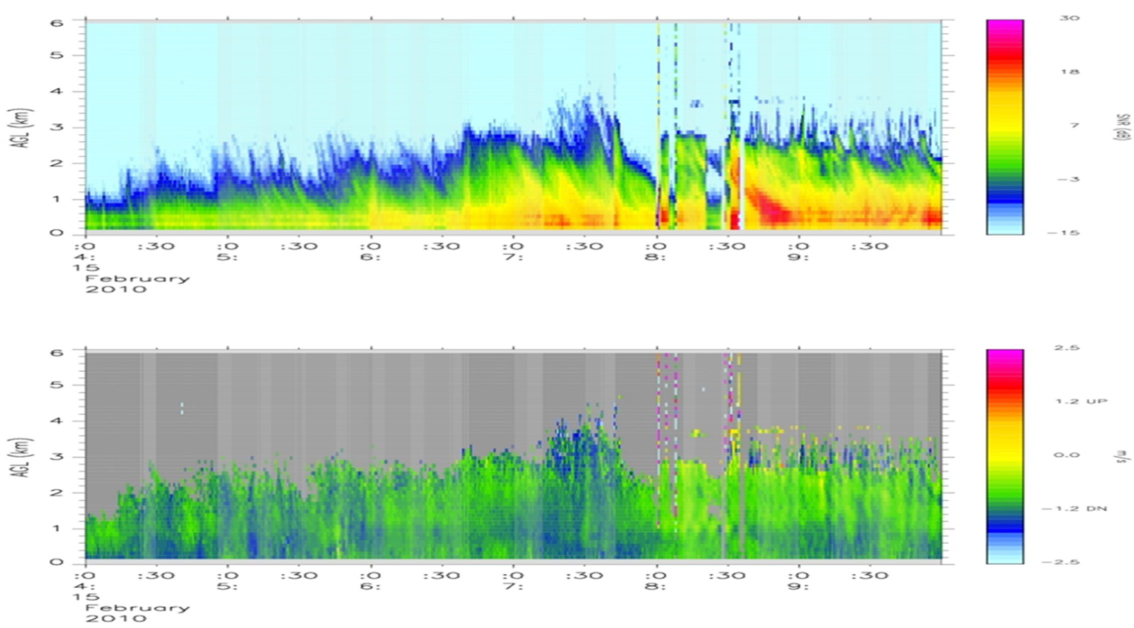

Figure 6: MIPS 915 MHz wind profiler Signal to noise ratio and vertical motion on February 15, from 0400-1000 UTC. Frontal Passage occurring at 0515 UTC

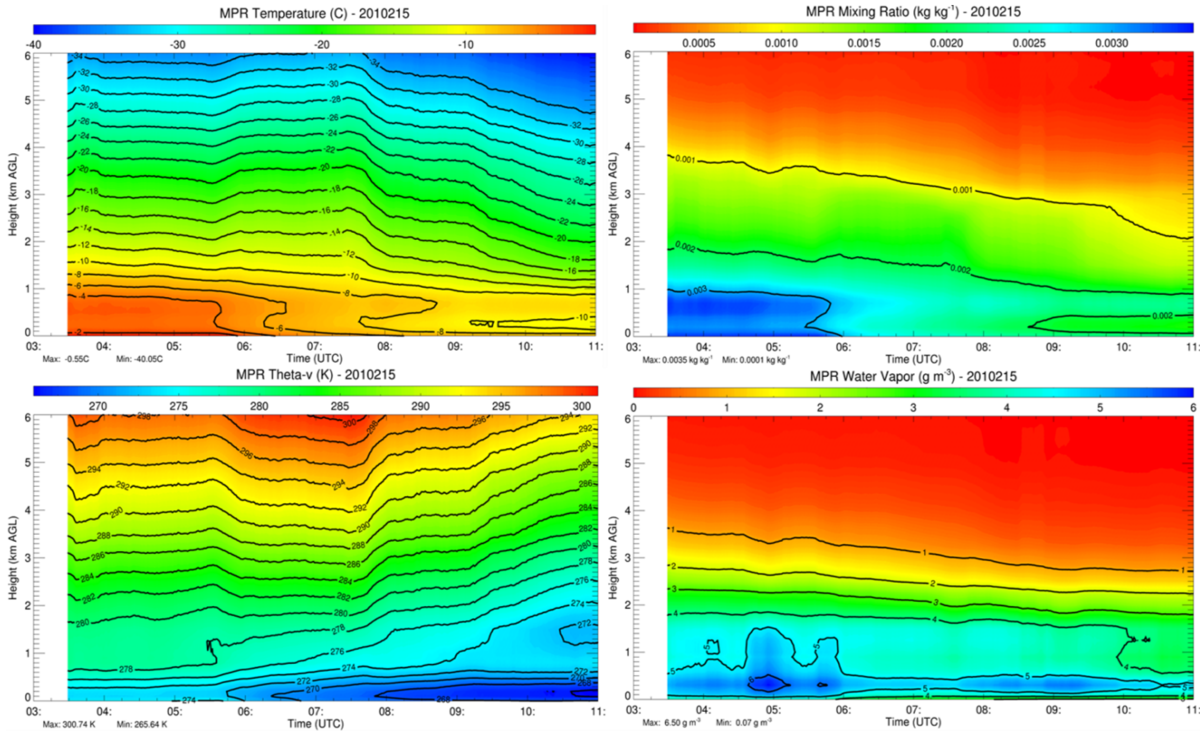

Figure 7: Top right: MPR Temperature Bottom Right: MPR Theta v Top Left: MPR Mixing Ratio Bottom Left: MPR Water Vapor from 0200-1000 UTC on the 15th. Passage of Shallow front at 0515 UTC and passage of upper level front at 0730

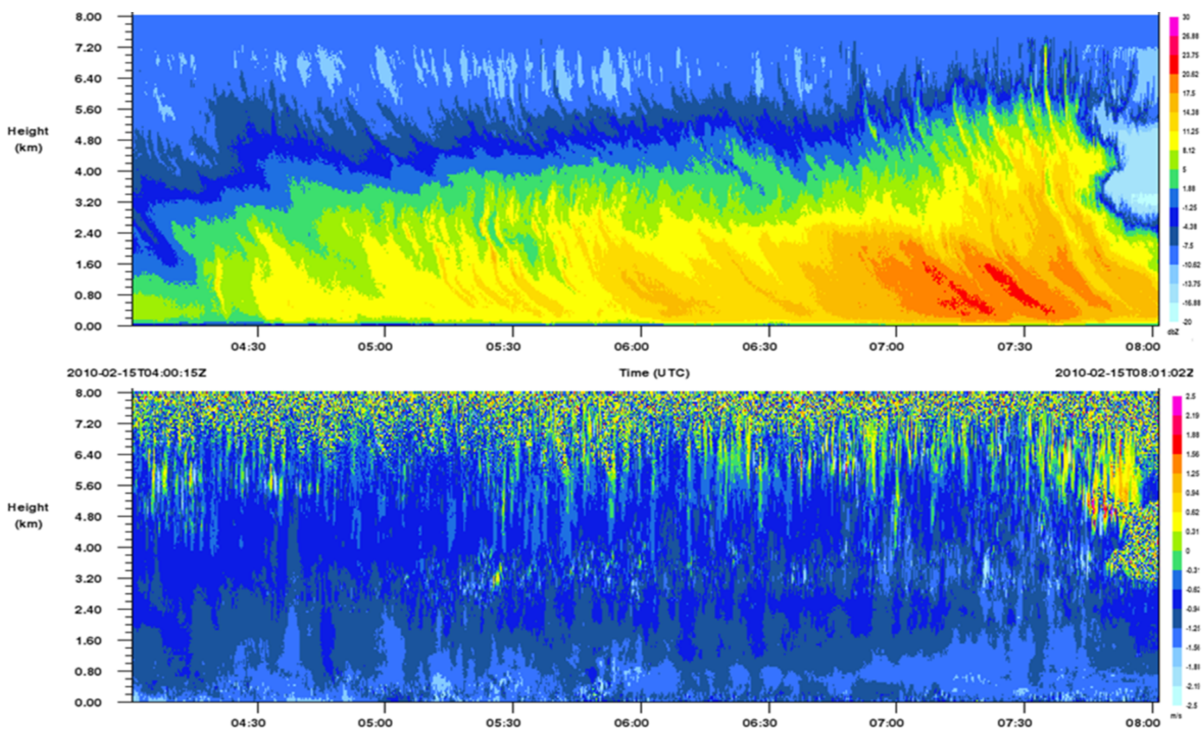

Figure 8: XPR Reflectivity and vertical motion from February 15 from 0400-0800 UTC. Frontal Passage occurring at 0515 UTC

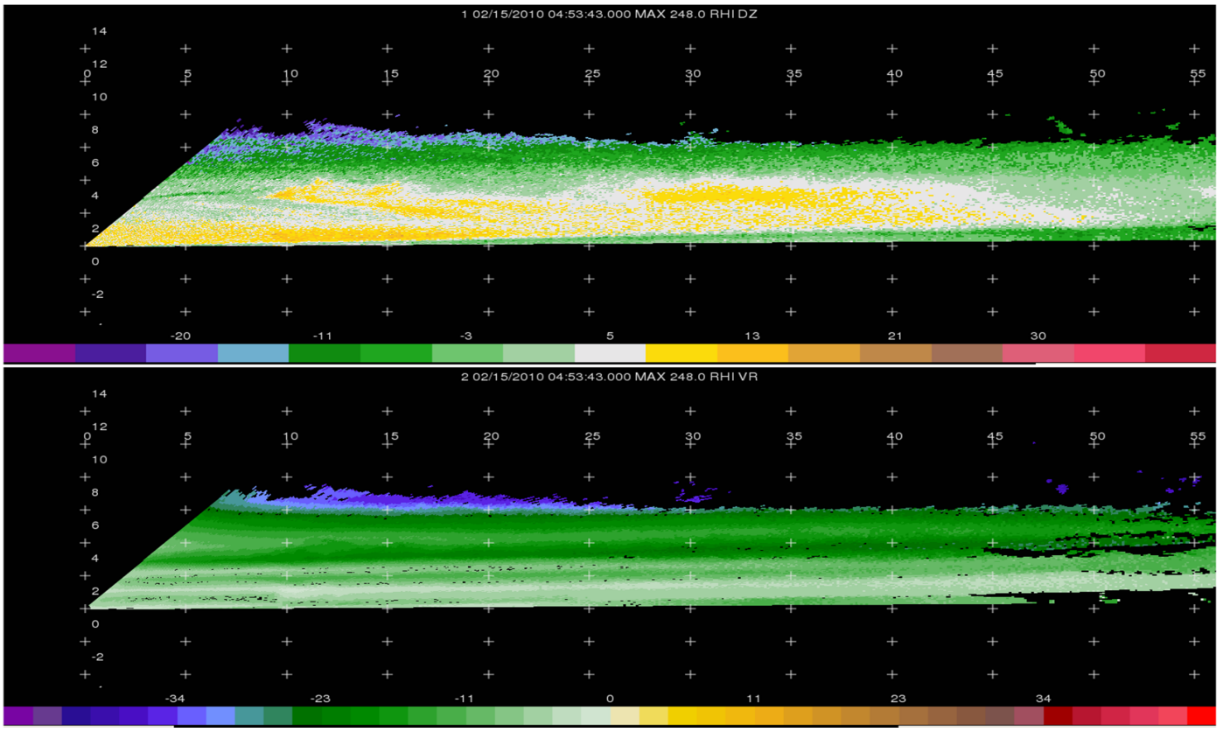

Figure 9: MAX prefrontal RHI from 248 degree azimuth at 0453 UTC showing reflectivity and velocity

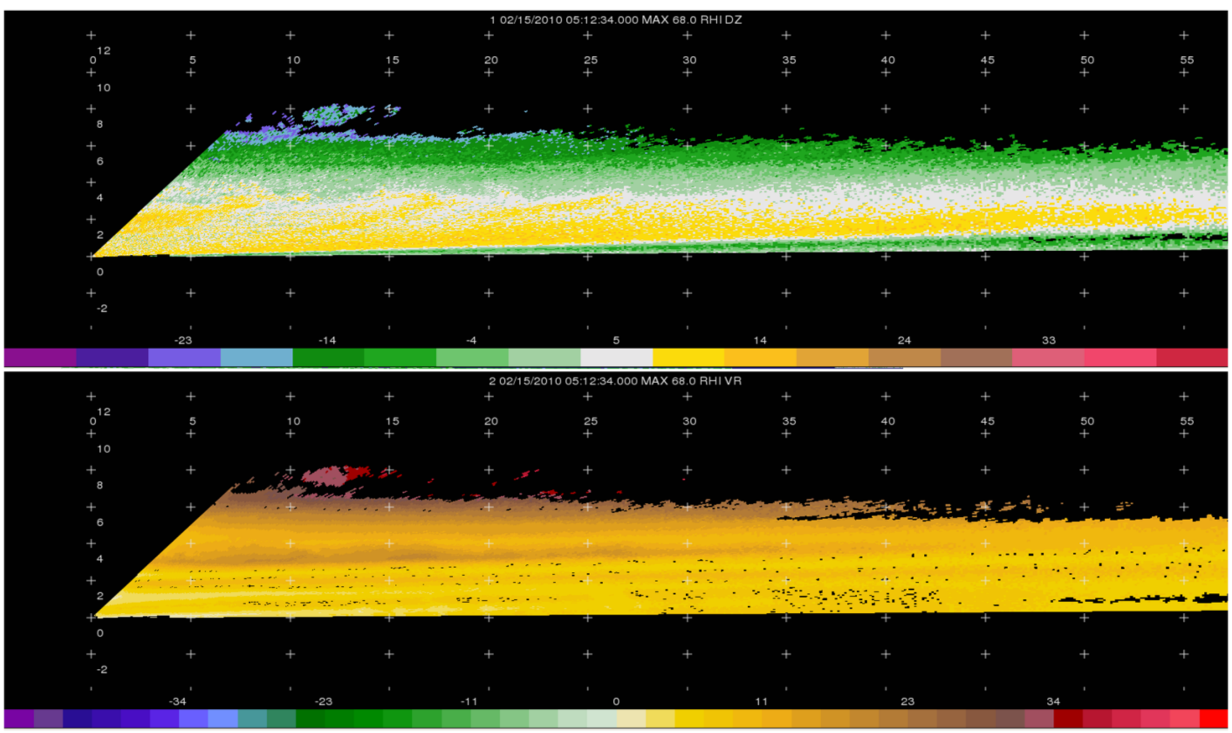

Figure 10: MAX postfrontal RHI from 68 degree azimuth at 0512 UTC showing reflectivity and velocity. RHI shows front around the time of it's passage over MIPS